

557-57  
82222

# THE EXTENSIONAL RHEOLOGY OF NON-NEWTONIAN MATERIALS

Stephen H. Spiegelberg and Gareth H. McKinley

Division of Engineering and Applied Sciences  
Harvard University  
Cambridge, MA 02138

6.9

## ABSTRACT

The evolution of the transient extensional stresses in dilute and semi-dilute viscoelastic polymer solutions are measured with a filament stretching rheometer of a design similar to that first introduced by Sridhar et al. (1991). The solutions are polystyrene-based (PS) Boger fluids that are stretched at constant strain rates ranging from  $0.6 \leq \dot{\epsilon}_0 \leq 4 \text{ s}^{-1}$  and to Hencky strains of  $\epsilon > 4$ . The test fluids all strain-harden and Trouton ratios exceeding 1000 are obtained at high strains. The experimental data strain-hardens at lower strain levels than predicted by bead-spring FENE models. In addition to measuring the transient tensile stress growth, we also monitor the decay of the tensile viscoelastic stress difference in the fluid column following cessation of uniaxial elongation as a function of the total imposed Hencky strain and the strain rate. The extensional stresses initially decay very rapidly upon cessation of uniaxial elongation followed by a slower viscoelastic relaxation, and deviate significantly from FENE relaxation predictions. The relaxation at long times  $t \geq 5 \text{ s}$ . is compromised by gravitational drainage leading to non-uniform filament profiles.

For the most elastic fluids, partial decohesion of the fluid filament from the endplates of the rheometer is observed in tests conducted at high strain rates. This elastic instability is initiated near the rigid endplate fixtures of the device and it results in the progressive breakup of the fluid column into individual threads or 'fibrils' with a regular azimuthal spacing. These fibrils elongate and bifurcate as the fluid sample is elongated further. Flow visualization experiments using a modified stretching device show that the instability develops as a consequence of an axisymmetry-breaking meniscus instability in the nonhomogeneous region of highly deformed fluid near the rigid endplate.

## INTRODUCTION

In recent years, concerted effort has been focused on the behavior of polymer solutions when subjected to strong extensional deformations. Extensional flows are found in most polymer-processing operations such as fiber-spinning, extrusion, and coating flows. Hence, rheological measurements of the appropriate materials under idealized extensional flow fields would be extremely valuable for comparison with theoretical model predictions. The parameter of interest is the uniaxial extensional stress growth coefficient  $\bar{\eta}^+$ , or the *transient extensional viscosity*, which is defined as

$$\tau_{zz}(t) - \tau_{rr}(t) = \bar{\eta}^+(t, \dot{\epsilon}_0) \dot{\epsilon}_0 \quad (1)$$

where  $\tau_{zz}(t) - \tau_{rr}(t)$  is the time-dependent normal or tensile stress difference, and  $\dot{\epsilon}_0$  is the constant imposed extensional strain rate. When the polymer chains reach maximum extension, the transient extensional viscosity reaches a constant steady-state value termed the *asymptotic extensional viscosity* denoted by  $\bar{\eta}(\dot{\epsilon}_0)$ .

Recent developments in extensional rheometer design have led to a greater understanding of the complexities of the behavior of polymer solutions in extensional flow. The filament stretching device first introduced by Cogswell [1] for melts has undergone several transformations throughout the years, the most significant recent contributions originating from Sridhar and co-workers [2, 3], who demonstrated the ability to generate a uniaxial extensional flow at a constant strain rate  $\dot{\epsilon}_0$  while measuring the small tensile forces exerted on the endplate by the deforming filament of fluid. In this design, a small, cylindrical sample of fluid is held between two rigid circular plates, which are then separated at a known rate. By measuring the force on one of the endplates, one can calculate the transient extensional viscosity growth function of the fluid as the Hencky strain  $\epsilon \equiv \dot{\epsilon}_0 t$  of the filament is increased.

With this design, Sridhar and co-workers have examined the extensional behavior of polyisobutylene-based Boger fluids [3] plus a shear-thinning polyisobutylene solution [4] and attained steady-state values in both systems.

The effects of the non-homogeneous kinematics on the measured material functions have been considered by Spiegelberg *et al.* [5]. Muller and co-workers [6] have examined the dependence of extensional behavior on solvent quality in polystyrene-based Boger fluids. In all these studies, the physical size of the sample and the minimum stretch rate attainable are constrained by gravitational body forces acting on the deforming filament, and the dimensionless quantity  $Bo/Ca = \rho g R_0^2 / \eta_0 \dot{\epsilon}_0$  must typically be less than unity. In a microgravity environment, larger samples and higher sample aspect ratios can be used which permit (i) the use of lower extension rates closer to the coil-stretch transition; (ii) larger sample aspect ratios that result in homogeneous kinematics, and (iii) application of other non-invasive diagnostic techniques for probing molecular structure, *e.g.* flow-induced birefringence.

In this paper we present ground-based measurements of the extensional viscosity for dilute polystyrene (PS) solutions obtained under normal gravitational conditions. These results are compared with models that predict the transient stress growth of pure elastic systems. These comparisons outline the need for microgravity conditions in order to further understand the complex response of these viscoelastic fluids in an extensional flow.

## EXPERIMENTAL

### *Test Fluid Rheology*

A series of three polystyrene-based Boger fluids with almost constant shear viscosities have been studied in the present work. High molecular weight polystyrene with a narrow polydispersity index (Scientific Polymer Products,  $M_w = 2.25 \times 10^6$  g/mole, P.D.I. = 1.02) was dissolved in oligomeric styrene (Hercules Piccolastic A5) with concentrations ranging from 0.05 wt.%  $< c < 0.2$  wt.% (500 – 2000 wppm). Simple molecular calculations for the high molecular weight PS species show that the critical concentration for chain overlap is  $c^* = 0.06$  wt.% [7] and the experimental test fluids therefore span the dilute and semi-dilute regime.

The viscometric material functions for these ‘Boger’ fluids were measured in a cone-and-plate geometry with a TA instruments controlled shear rheometer and have been discussed in detail elsewhere [5]. The viscometric properties of the fluids in steady and transient shear-flows can be quantitatively described by the bead-spring model of Zimm and can also be approximately modeled in strong flows by the simpler Chilcott-Rallison constitutive equation. In this model, the dilute solution of monodisperse polystyrene chains are considered to act as a non-interacting suspension of dumbbells connected by a finitely extensible nonlinear elastic (FENE) spring. The finite extensibility of the dumbbells is estimated to be  $L \approx 37$  by using the specified molecular properties of the monodisperse polystyrene to calculate the r.m.s. length and contour length of the statistically equivalent freely-jointed Kuhn (bead-rod) chain [5]. The key viscometric parameters for all three fluids, along with the oligomeric styrene forming the athermal, viscous Newtonian solvent, are listed in Table I.

### *Experimental Apparatus*

The filament-stretching rheometer used in this work is described in detail in [5]. Tests were conducted in air under normal gravitational conditions at  $T = 25$  °C. Small samples with an initial diameter  $D_0 = 0.3$  or  $0.7$  cm and lengths ranging from  $0.05 \leq L_0 \leq 0.3$  cm were used to ensure that for the sample at rest, surface tension forces would dominate gravitational body forces. An example of the sequence of video-images obtained from the extensional deformation of a non-Newtonian fluid sample is shown in Figure 1. Modified endplate velocity profiles were used to ensure a constant effective strain rate as measured from the minimum diameter [3, 5]. The latter approach is used to compensate for the no-slip boundary conditions that exist at the fixed endplates and the resulting nonhomogeneous kinematics that arise at short times. Upon completion of stretching, the force on the bottom plate was monitored until significant gravitational drainage was apparent. For the strongly strain-hardening materials examined here, the force could be monitored for 2-3 seconds. As we discuss below, these measurements provide valuable information about the relaxation behavior of the polymer chains from an initial configuration close to full extension, and provide an indication of the relaxation spectrum of the material.

## RESULTS AND DISCUSSION

Experimental results for a Newtonian polystyrene oil ( $\dot{\epsilon}_0 = 4.5$  s<sup>-1</sup>) and a non-Newtonian 0.05 wt.% PS/PS Boger fluid solution ( $\dot{\epsilon}_0 = 3.3$  s<sup>-1</sup>,  $De = 2.8$ ) subjected to an extensional deformation are shown in Figure 2, where the transient Trouton ratio  $Tr \equiv \bar{\eta}^+ / \eta_0$  is plotted as a function of the Hencky strain  $\epsilon$ . The results demonstrate that the response of the non-Newtonian fluid is initially very similar to the Newtonian oil for strains  $\epsilon < 2$ . At higher levels of stretch, the polymer molecules approach maximum extension, the connector force between the chain ends becomes increasing nonlinear and the polymer chains begin to undergo non-affine

deformation. The fluid stress begins to rise, and increases several orders of magnitude at high Hencky strains. In the Newtonian fluid, however, the dimensionless stress approaches a constant value of  $Tr = 3$ , and remains invariant with Hencky strain. The initial overshoot in both fluids is a result of the non-ideal flow kinematics which occur at the solid endplates [5], and is well-described by the one-dimensional model shown with the experimental data.

The non-Newtonian predictions for two simple constitutive models are shown together with the experimental data in Figure 2. The polymer chain is considered to be a simple dumbbell in both models. The Oldroyd-B model assumes that the polymer chain is infinitely extensible ( $L \rightarrow \infty$ ) and the extensional viscosity increases without bound. The Chilcott-Rallison model incorporates finite chain extensibility and the Trouton ratio is predicted to approach an asymptotic value that scales as  $\bar{\eta} \sim L^2$ . Both models underpredict the transient response observed in the experimental data, which grows at a rate faster than that expected from affine extensional deformation of a Hookean dumbbell. It is possible that there is an additional 'viscous' or dissipative contribution to the total tensile stress in the fluid which arises from conformation-dependent drag on the deforming polymer chains [9], and which is not captured by simple FENE models that only account for the recoverable 'elastic' contribution to the stress arising from the loss of configurational entropy of the polymer chains. An alternative explanation is that the internal relaxation modes of the actual macromolecule give rise to a spectrum of relaxation times which lead to modifications of the dynamical processes by which the chains unravel during transient uniaxial elongation.

The discrepancy between the theoretical predictions and experimental results leads to the need for two additional sets of measurements to be conducted during the extensional test. Firstly, to decouple the two sources of measured stress, an independent measure of the microstructural deformation at the molecular-level is required. Phase-modulated birefringence measurements can provide the appropriate time-resolved non-invasive indication of the degree of orientation of the polymer chains [10]. As the degree of orientation is directly related to the level of elastic or 'entropic' stress experienced by the polymer chains, *in situ* birefringence measurements will probe the elastic contribution to the total measured stress, and the measured response should compare well with the FENE models.

Secondly, in addition to birefringence measurements, it is instructive to monitor the stress relaxation behavior of the polymer chains upon cessation of flow. As the deformation stops, any viscous or 'dissipative' component of the measured stress should disappear immediately, followed by a gradual viscoelastic decay of the residual elastic stresses. This stress relaxation may be measured both with birefringence and independently with the overall endplate force measurement. An example of stress relaxation following extensional deformation is shown in Figure 4 for a 0.05 wt.% PS/PS solution stretched at a single fixed extension rate to differing levels of strain. For comparison, the relaxation prediction of the Chilcott-Rallison model for a strain level of  $\varepsilon = 4.08$  is also shown. The single mode relaxation predicted by the CR model decreases at a much lower rate than the experimental results. The initial drop in stress is convoluted with the deceleration time of the mechanical system; thus it is unclear at present if the initial drop is instantaneous or has a small finite relaxation time. In either case, it is evident from these preliminary results that a single-relaxation mode model lacking any viscous component is insufficient to predict the relaxation behavior of these materials when subjected to a strong extensional flow.

Both of the latter experiments are complicated by the presence of gravitational body forces. To make successful birefringence measurements, samples with large initial radii are required to prevent refraction of the polarized laser light beam that passes through the deforming column. As the diameter increases, however, the susceptibility of the fluid column to gravitational sag increases dramatically. Similarly, analysis of the stress relaxation studies require that a uniform cylindrical fluid column is maintained for several seconds. As the stress relaxes in the fluid, however, the fluid motion begins to reverse as the sample drains away from the upper plate under the influence of gravity. Therefore, for successful completion of these tests and hence complete understanding of the behavior of these materials under extensional deformation, access to an extended reduced-gravity environment is required.

An additional complication in the measurements of extensional viscosity results from the endplate conditions. As we have reported in [5], the rigid endplates lead to the partial decohesion of the filament from the endplates. A rigorous investigation shows that the axial curvature of the fluid filament at the endplates and the resulting adverse pressure gradient in the fluid lead to the formation of an elastic instability, which grows as the Hencky strain increases [11]. This instability only appears in samples that exhibit significant strain-hardening; however, the instability can lead to erroneous interpretation of the experimental data, as the appearance of the instability coincides with a leveling of the measured stress, which under normal circumstances could be interpreted as the attainment of steady-state extension. Two images at the onset of the instability are shown in Figure 4. The first image shows an axial side view of a 0.05 wt.% solution subjected to a strain rate  $\dot{\varepsilon}_0 = 2 \text{ s}^{-1}$  after a strain of  $\varepsilon \approx 4.3$ . The second image shows the spatial plan-form of the non-axisymmetric disturbance to the free-surface of the fluid

column using a camera that is focused axially upwards through a lower plate made of glass. At the onset of the instability, the cylindrical column breaks up into 3-5 lobes typically, which grow in a dendritic pattern exhibiting 'tip-splitting' and the formation of tertiary side-lobes.

Although this phenomenon is hydrodynamically interesting, it results in nonhomogeneous fluid deformations and prohibits determination of the extensional viscosity of the material. Such disturbances can not be eliminated by microgravity conditions, and in order to prevent onset of such elastic instabilities, it is necessary to impose the correct fluid boundary conditions at the endplates of the test device. Following the concept proposed and implemented by Kröger *et al.*[12], 'adaptive endplates' are being constructed that will inhibit axial curvature of the fluid interface at the endplates, and will thus eliminate the dynamical mechanism for instability.

## CONCLUSIONS

Ground-based experimental measurements of extensional viscosities for polystyrene-based viscoelastic solutions demonstrate a large increase in the transient extensional viscosity with strain, and dimensionless Trouton ratios increasing by three orders of magnitude. Comparisons with FENE models demonstrate that the single mode models do not capture the rapid increase in tensile stress with Hencky strain. Simultaneous birefringence measurements, coupled with stress relaxation studies following extension, will provide further information regarding the source of the discrepancy between model and experiment. Non-idealities in the flow characteristics of the filament-stretching rheometer result in partial decohesion of highly strain-hardening fluids. The non-idealities may be addressed with an adaptive endplate that imposes the correct radial velocity, rendering the fluid sample a cylinder for the majority of the test.

## REFERENCES

- (1) Cogswell, F. N. *Plast. Polym.*, **36**, 109 (1968).
- (2) Sridhar, T.; Tirtaatmadja, V.; Nguyen, D. A.; Gupta, R. K. *J. Non-Newtonian Fluid Mech.*, **40**, 271-280 (1991).
- (3) Tirtaatmadja, V.; Sridhar, T. *J. Rheol.*, **37**, 1081 (1993).
- (4) Ooi, Y. W.; Sridhar, T. *J. Non-Newtonian Fluid Mech.*, **52**, 153-162 (1994).
- (5) Spiegelberg, S. H.; Ables, D. C.; McKinley, G. H. *J. Non-Newtonian Fluid Mech.*, **to appear**, (1996).
- (6) Solomon, M. J.; Muller, S. J. *submitted to J. Rheology*, (1996).
- (7) Flory, P. J. *Principles of Polymer Chemistry*; Cornell University Press: Ithaca, 1953.
- (8) James, D. F.; Sridhar, T. *J. Rheol.*, **39**, 713-724 (1995).
- (9) Hinch, E. J. *J. Non-Newtonian Fluid Mech.*, **54**, 209-230 (1994).
- (10) Fuller, G. G. *Ann. Rev. Fluid Mech.*, **22**, 387-417 (1990).
- (11) Spiegelberg, S. H.; McKinley, G. H. *J. Non-Newtonian Fluid Mech.*, **to appear**, (1996).
- (12) Berg, S.; Kröger, R.; Rath, H. J. *J. Non-Newtonian Fluid Mech.*, **55**, 307-319 (1994).

Table 1. Zero-shear rate viscometric properties for three polystyrene-based Boger fluids denoted PS-05 (0.05 wt.%), PS-1 (0.1 wt.%), and PS-2 (0.2 wt.%) and a viscous polystyrene (PS) oil. All data at  $T_0 = 25^\circ\text{C}$ .

Measured Material Property	PS-05	PS-1	PS-2	PS Oil
$\eta_0$ [Pa.s]	47.7	52.0	70.4	
$\eta_s$ [Pa.s]	37.2	37.9	36.7	37.0
$\Psi_{10}$ [Pa.s <sup>2</sup> ]	18.3	42.5	122.6	
$\sigma$ [N/m]	$29 \times 10^{-3}$	$29 \times 10^{-3}$	$29 \times 10^{-3}$	$29 \times 10^{-3}$
Computed Model Parameters				
$\lambda_s = \Psi_1 / 2(\eta_0 - \eta_s)$ [s]	0.87	1.52	1.82	
$\beta = \eta_s / \eta_0$	0.78	0.73	0.52	

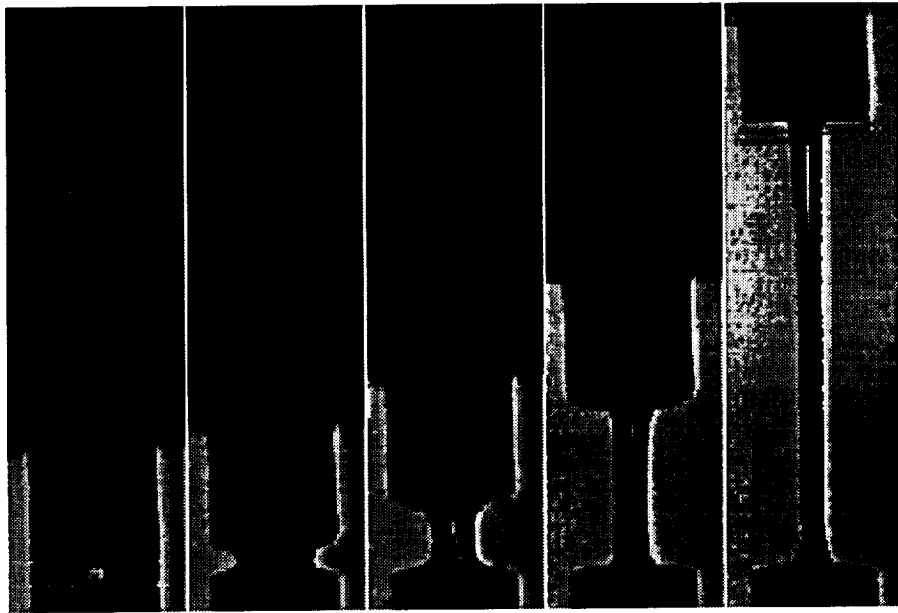


Figure 1: Evolution of a cylindrical fluid sample of 0.05 wt.% PS/PS solution stretched at a constant strain rate  $\dot{\epsilon}_0 = 2.0 \text{ s}^{-1}$ , corresponding to  $De = 1.4$ . Images are spaced 0.4 seconds apart. Sample aspect ratio  $\Lambda_0 = L_0/R_0 = 0.33$ , where  $R_0 = 0.15 \text{ cm}$ . The dashed lines show the initial sample length  $L_0$ .

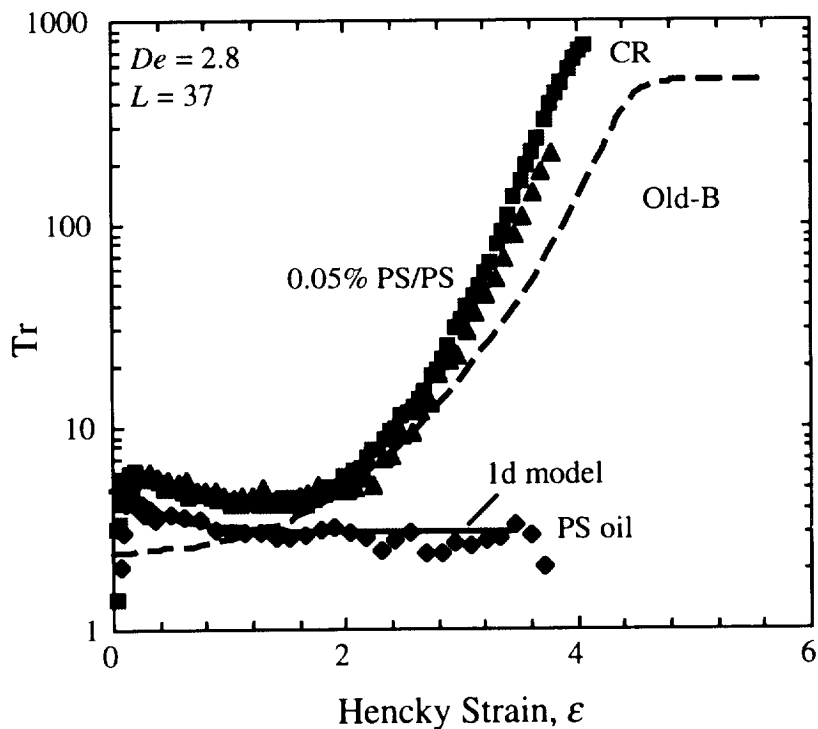


Figure 2: Strain-hardening in the transient tensile stress growth coefficient ( $Tr = \bar{\eta}^+ / \eta_0$ ) of 0.05 wt.% PS/PS solutions stretched at a Deborah number  $De = 2.8$ . The predictions for two dumbbell-like models are shown for comparison, together with the response for a Newtonian PS oil.

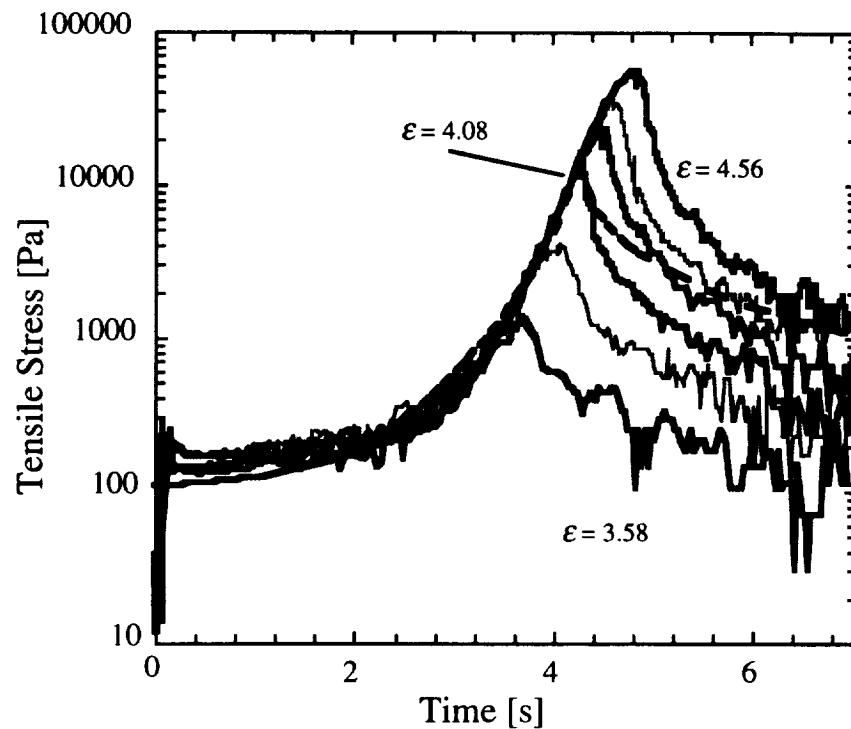


Figure 3: Stress relaxation behavior of 0.05 wt.% PS/PS solutions subjected to the same extensional strain rate  $\dot{\epsilon}_0 = 0.92 \text{ s}^{-1}$  for Hencky strains  $\epsilon = 3.58, 3.87, 4.08, 4.29, 4.32,$  and  $4.56$ . The relaxation behavior of the Chilcott-Rallison model for  $\epsilon = 4.08$  is shown for comparison as a dashed line.

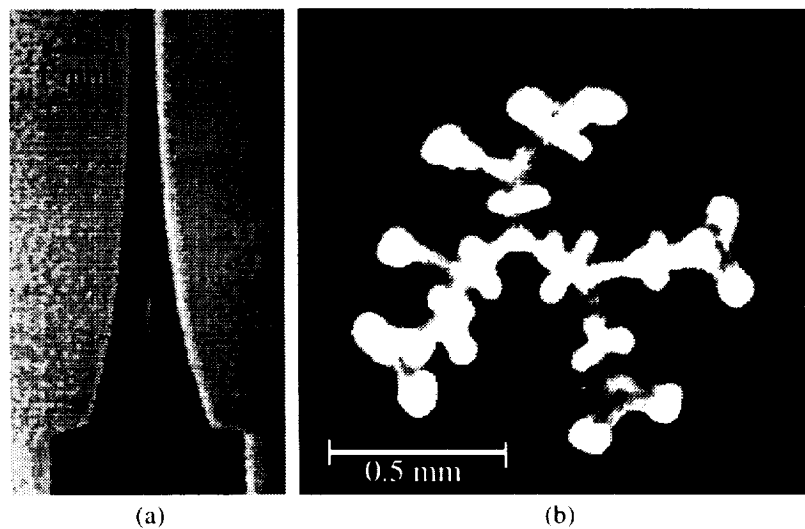


Figure 4: Onset of elastic instability in 0.05 wt.% PS/PS solution in extensional flow,  $\epsilon = 4.6$  and  $\dot{\epsilon}_0 = 2.0 \text{ s}^{-1}$  for  $\Lambda_0 = L_0/R_0 = 0.33$ . (a) Side view, (b) plan view. Images are taken from 2 different experiments at identical kinematic conditions.